Phase transition and surface morphology of MnAs/GaAs(001) studied with *in situ* variable-temperature scanning tunneling microscopy

R. Breitwieser,[1,2] F. Vidal,[1] I. L. Graff,[1,*] M. Marangolo,[1] M. Eddrief,[1] J.-C. Boulliard,[3] and V. H. Etgens[1]
[1]*Institut des NanoSciences de Paris, UPMC, CNRS UMR 7588, 140 rue de Lourmel, 75015 Paris, France*
[2]*LCPMR, UPMC, CNRS UMR 7614, 11 rue Pierre et Marie Curie, 75005 Paris, France*
[3]*IMPMC, UPMC, CNRS UMR 7590, 140 rue de Lourmel, 75015 Paris, France*
(Received 21 January 2009; revised manuscript received 5 May 2009; published 6 July 2009)

The MnAs phase transition from the hexagonal ferromagnetic α to the orthorhombic paramagnetic β phase has been investigated *in situ* by variable-temperature scanning tunneling microscopy (STM) as a function of epilayer thickness. The α-β phase coexistence leads to the formation of a self-organized stripes pattern of alternating α and β regions. The morphology evolution of the α-β periodic array of domains has been imaged in detail. The period and corrugation of this pattern are linear functions of the epilayer thickness with a domain periodicity nearly five times larger than film thickness. Also, STM local imaging through the phase-coexistence region (10–45 °C) shows unambiguously the absence of mass transport during the transition. The self-organization of α-β stripes is consistent with an elastic-energy equilibrium state of the heteroepitaxial system at each temperature, as previously proposed for the origin of the modulated structure [V. M. Kaganer *et al.*, Phys. Rev. B **66**, 045305 (2002)]. Independently of self-organized α-β regions, the surface displays anisotropic mounds that are elongated along MnAs *a* axis. This facetting process leads to a peculiar, highly anisotropic surface with oriented facets and submicron periodic modulation along the hexagonal *c* axis. Smoother surfaces with larger terraces are obtained following postgrowth annealing. These results suggest that a careful control of the growth temperature and annealing procedure can be used to tailor the surface morphology for specific applications requiring anisotropic templates.

DOI: 10.1103/PhysRevB.80.045403 PACS number(s): 68.37.Ef, 68.55.A−, 68.55.J−

I. INTRODUCTION

Manganese arsenide (MnAs) is a metallic material exhibiting an unusual sequence of polymorphic transformations.[1,2] At low temperature, bulk MnAs has a hexagonal NiAs-type structure (α phase) and is ferromagnetic. A first-order phase transition occurs at 40 °C toward a paramagnetic orthorhombic MnP-type structure (β phase). Further increase in the temperature leads to a second-order phase transition at 127 °C with the recovering of the hexagonal NiAs-type structure in a paramagnetic state (γ phase). Due to its compatibility with standard semiconducting substrates[3–7] and a strong spin polarization,[8,9] the interest on this compound has been renewed recently in the framework of spintronics. Many studies have been performed on the structural, magnetic, and transport properties of MnAs epilayers grown on GaAs substrates. It was found that the α-β phase transition is strongly perturbed in epilayers as compared to bulk.[10–12] The transition-temperature range is extended with coexistence of α and β phases as a consequence of the constraints imposed by the epitaxy. On GaAs(001), the α and β phases coexist between 10 and 45 °C.[10] This phenomenon has been extensively studied in recent years by x-ray diffraction, x-ray scattering, optical spectroscopy, and scanning probe microscopy (SPM).[6,10,13–19] SPM imaging revealed the existence of ridges and grooves organized in stripe-shaped domains with alternating α and β regions (see scheme in Fig. 1). The origin of the phase coexistence has been previously proposed to lie in the markedly distinct thermal expansion of MnAs and GaAs, which leads to a minimization of the elastic energy through α-β coexistence over an extended temperature range.[10] The reported values for the amplitude of the modulation (i.e., the height difference between α and β regions) available in the literature show a strong scattering. Some studies report a 5–6 % difference[14] which seems excessive in the framework of an elastic deformation but that could be

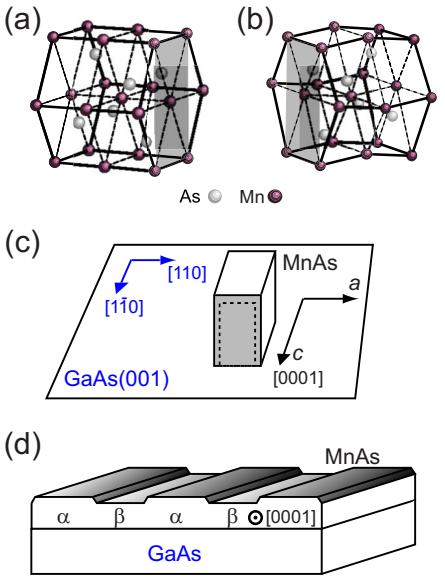

FIG. 1. (Color online) (a) Hexagonal cell of α-MnAs. (b) Orthorhombic cell of β-MnAs. (c) Scheme for the MnAs/GaAs(001) epitaxy. The basal plane (orthorhombic cell of MnAs with the basal plane in gray) is perpendicular to the surface and MnAs [0001] direction parallel to [1$\bar{1}$0] direction of GaAs. The dashed line within the basal plane illustrates the deformation of the orthorhombic β phase. (d) Schematic view of the α-β-stripes organization.

 ©2009 The American Physical Society

easily explained if mass transport across the epilayer was involved in the process. However the very existence of an important mass transport operating in the vicinity of room temperature is hard to conceive. In such a context, a real-space *in situ* study of the MnAs/GaAs(001) surface morphology as a function of the temperature could bring an ultimate clue on the origin of the α-β modulation. Moreover, considering the potential use of this epilayer as a temperature-tunable template,[20] the study of the surface morphology is of primary importance. Surprisingly, despite numerous studies on the properties of MnAs/GaAs(001) epilayers, investigations using variable-temperature scanning tunneling microscopy (VT-STM) have not been reported so far. In this paper we report on the study of the surface morphology of MnAs/GaAs(001) using a variable-temperature STM apparatus directly connected through ultrahigh vacuum (UHV) to the molecular beam epitaxy (MBE) chamber. The surface structure was probed as a function of the temperature at several scales from microns down to nanometer to access both the thermal evolution of the phase-coexistence modulation and the detailed surface morphology. The main goals of our work consist in: (i) clarifying, by a direct measurement (STM), if a mass-transport mechanism could be responsible for the morphology of α-β-stripes pattern and (ii) examining in details the morphology evolution during the phase transition at a lower scale down to nanometer.

II. EXPERIMENT

MnAs epilayers were grown by MBE on GaAs(001) substrates. Epiready GaAs substrates were first deoxidized under As overpressure followed by a GaAs buffer-layer growth in standard growth conditions. At the end, the surface was long annealed at 600 °C under As to optimize its quality, confirmed by the presence of a clear $(2\times4)\beta$ diagram as checked by reflection high-energy electron diffraction (RHEED). Next, we have cooled down the sample and followed the procedure of Arai *et al.*[21] to obtain a stable and high-quality As-terminated $c(4\times4)$ surface. The MnAs growth was performed at 260 °C under As-rich conditions and a growth rate of about 3 nm/min. The epitaxial relationship was first verified *in situ* by RHEED and crosschecked *ex situ* by x-ray diffraction. MnAs displayed a single domain epitaxy from the beginning of the growth with $[0001]_{\mathrm{MnAs}}\|[1\bar{1}0]_{\mathrm{GaAs}}$, as illustrated in Fig. 1. Samples were then immediately transferred to the variable-temperature STM apparatus (VT-STM from Omicron NanoTechnology GmbH) connected to the MBE setup, thereby allowing UHV transfer of the samples. The images presented in this work were obtained in constant current mode. The sample temperature was varied between −100 and +60 °C as monitored by a Pt-100 resistor. STM images were treated and analyzed using WSXM software.[22] Samples thickness determination was performed using x-ray reflectivity and transmission electron microscopy.

III. RESULTS AND DISCUSSION

A. α-β domains

Images collected within the micron scale, where the alternating α-β-stripes pattern can be clearly observed, are described first. Figure 2 depicts, for a 280-nm-thick MnAs epilayer, a typical surface-morphology evolution during the α-β phase transition. The groove-ridge structure running along [0001] MnAs direction is visible in Fig. 2(b) for a temperature inside the coexistence window. Bright regions correspond to the α phase while the β phase (lower position with respect to α) looks dark. The height difference between α and β phases can be quantitatively appreciated on the profiles depicted in Fig. 2(d): 0 °C (pure α phase), 27 °C (α-β coexistence), and 54 °C (pure β phase). While the pure phases exhibit a stripe-free surface, the amplitude of the modulation reaches 3 nm at 27 °C.

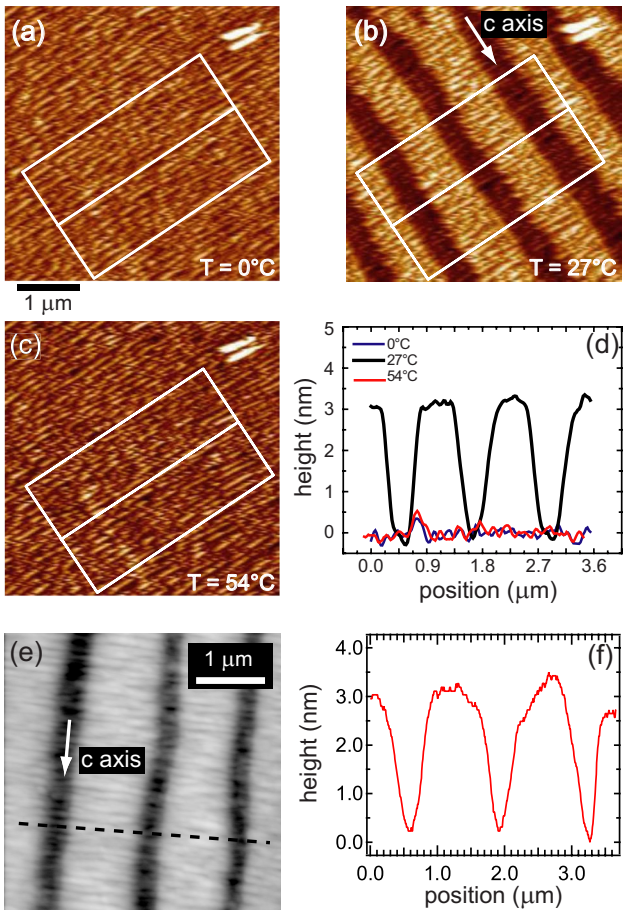

FIG. 2. (Color online) (a)–(c) 4.4×4.4 μm^2 STM images of a 280-nm-thick MnAs epilayer obtained in constant current mode (I=0.3 nA, V_{bias}=0.8 V) for three temperatures (T=0 °C, pure α phase; T=27 °C, α-β-stripes pattern; and T=54 °C, pure β phase). (d) Averaged height profiles corresponding to the white rectangles in (a)–(c). (e) AFM image (4.0×4.0 μm^2) obtained *ex situ* at room temperature. (f) Profile obtained along the dashed line in (e).

The evolution of this organized pattern with MnAs thickness (t) is resumed in Fig. 3 where period (λ) and average height differences between α and β domains (h) are plotted as a function of t. Measurements were performed in the 70–280-nm-thickness range. λ and h are found to be linear functions of t with the following relationships: $\lambda\approx4.8t$ and $h\approx0.01t$. The linearity of λ with respect to thickness was already observed by Kästner *et al.*[14]

Kaganer *et al.*[10] showed that the α-β coexistence is a consequence of energy minimization mediated by an elastic-

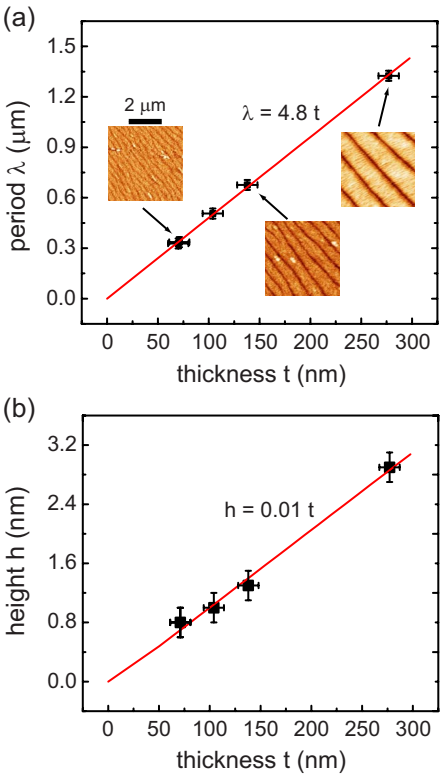

FIG. 3. (Color online) (a) Period of the α-β-stripes pattern in the coexistence region as a function of the MnAs-epilayer thickness. Insets are characteristic STM images obtained in constant current mode. (b) Averaged height difference between α and β regions, as a function of the MnAs-epilayer thickness.

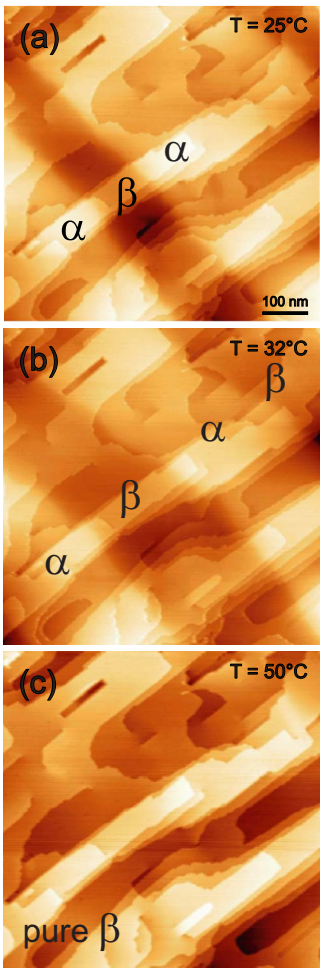

FIG. 4. (Color online) (a)–(c) Sequence of STM images (700 $\times$700 nm^2, I=0.5 nA, V_{bias}=0.8 V) taken during temperature cycling across the α-β phase transition, showing the absence of mass transport across the phase-coexistence region. MnAs thickness: 105 nm.

modulation process. The large lattice misfit between MnAs and GaAs is released at early stages of the growth by the formation of a series of misfit dislocations at the interface.[23] However, GaAs and MnAs have markedly different linear dilatation coefficients that lead to thermal strain during the cooling step after growth. In bulk MnAs at the phase transition, the lattice parameter increases softly with temperature along the hexagonal c axis, while it shows a sharp and discontinuous variation in the basal plane (decrease of about 1%) that implies a volume shrink of $\sim$2%. In an epilayer, the lateral size is clamped by the substrate that induces an in-plane biaxial anisotropic strain while the out-of-plane parameter (along the growth direction) is free to relax. When heating the epilayer initially in the α phase, the premature appearance of the β phase helps the system to release its strain and so, to minimize its energy. Elastic modeling of this phenomenon has been already used to explain the periodic organization into alternating α and β domains where the elastic-energy density depends only on the domain size, on the α-β phase fraction, and on the difference in internal strain between the two phases. Such calculations, performed in details by Kaganer *et al.*,[10] showed that the period of the stripes is wide if the strain is localized essentially in the vicinity of the α-β boundaries. In the framework of this model, large α and β domains ensure that the elastic strains in the direction normal to the film-substrate interface relax independently in the two phases. Narrow domains, on the other hand, tend to reduce the elastic strain at the interface with the substrate. However, in such a case, the two phases are strained and adopt equal α-β lattice spacing in the direction normal to the film-substrate interface. The competition between these two driving forces results in a periodic modulation of the film thickness[14] with a period λ proportional to the film thickness t ($\lambda \sim 5.6t$ when the α/β phase fraction varies between 20 and 80%, in the model calculations[10]).

In the case of an elastic-induced self-organization phenomenon, no mass transport but only minute deformations are expected and the relative height difference between α and β phases [approximately 1%, given in Fig. 2(d)] should be equal to the lattice mismatch between α and β MnAs in the growth direction. X-ray diffraction measurements give a $\sim$1.1% mismatch along the growth direction in the phase-coexistence region,[13] in very good agreement with the present measurements. We note that the α-β corrugation amplitude measured by STM [3 nm for 280-nm-thick layer, see Fig. 2(d)] is smaller than the one measured by atomic force microscopy (AFM) in Ref. 14 (5 nm for a 95-nm-thick layer and 8 nm for 130 nm). To check this discrepancy, we have performed *ex situ* AFM measurements on the same uncapped

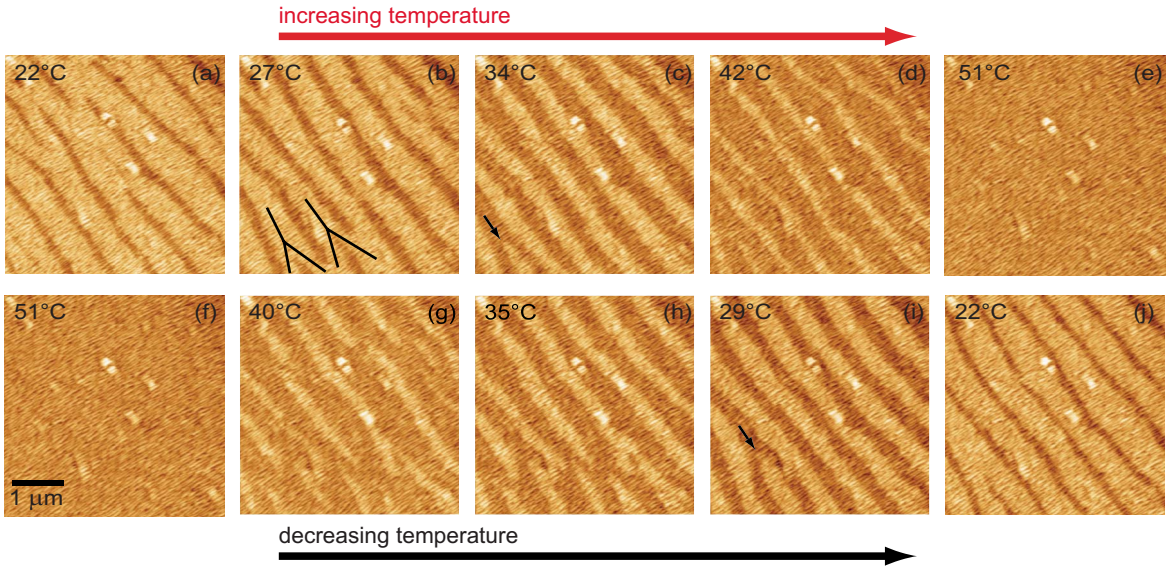

FIG. 5. (Color online) (a)–(j) Sequence of STM images (4.2×4.2 μm^2, I=0.5 nA, V_{bias}=0.8 V) taken during temperature cycling across the α-β phase transition. The temperature was increased up to 60 °C in the pure β temperature range before imaging the surface during lowering of the temperature. Each image has been taken in the same region, as witnessed by the three bright defects in the center of the images.

sample measured by STM. The results [Fig. 2(e) and 2(f)] confirm the ~1% height difference between α and β regions seen in our STM measurements. So, the α-β surface corrugation-thickness dependence (~1%) and the periods evolution (for film thickness in the 70–280 nm range) reported in Fig. 3 are fully consistent with the elastic origin of the stripes pattern. This suggests that the large corrugation amplitudes reported previously in Ref. 14 are likely due to measurement errors.

Next, we address the mass-transport question after analysis of high-resolution images. Nanometer-scale STM images showing the steps shape and distribution of a given surface, performed at different temperatures in the phase-transition temperature interval, can unambiguously resolve if mass transport occurs. Such analysis can then definitely discriminate between elastic deformation and mass transport as one of the origin of the domains. Figure 4 shows the same region at three different temperatures during the phase transition. The surface morphology remains completely independent of the domains across the phase transition with no evolution of the terraces, steps, and kinks in the coexistence region while the lateral size of the β phase increases. This direct (i.e., real-space local imaging across the temperature interval of phase coexistence) observation rules out definitively mass transport in the phase-coexistence interval.

Considering the potential use of the MnAs α-β pattern as a template for further growth of temperature-tunable structures,[20] its robustness during temperature cycling deserves further investigation. Figure 5 depicts a sequence of STM images obtained in the same region, for a 140-nm-thick MnAs epilayer, during temperature cycling. At higher temperatures, coming from pure β phase [40 °C, Fig. 5(g)], finite-length α stripes nucleate with a wavy shape until interconnection occurs. The most regular arrangement is obtained for equal α/β proportions. At both ends of the coexistence region, registry faults are present and antiphase stripes coalesce, forming Y-shaped junctions [Fig. 5(b)]. Such defects were observed in AFM measurements performed at room temperature.[24] In the framework of the elastic model,[10] the periodic strain should lead to a regular parallel arrangement of domains, emerging, and collapsing at the same place but the real situation is more complex. After cycling the temperature, a similar arrangement is recovered for equal proportions of α and β, as shown by STM images (c) and (i) in Fig. 5. While the upper right corner of the images looks quite similar, an interrupted domain has changed position in the lower left corner, as marked by black arrows. Such a fault could reflect the instability caused by the merging of two neighboring Y-shaped junctions linking 4 α domains, see lower left corner of Fig. 5(b). We attribute such behavior to the fact that a periodic strain field developing in a real crystal, i.e., with defects such as dislocations, can be substantially affected by local perturbations. In bulk MnAs, the first-order α/β phase transition proceeds with a marked thermal hysteresis. This means that the stripes pattern may also be affected by the thermal history of the sample. The α/β proportion depends on the temperature and on the variation sense of the temperature, i.e., for a given temperature the stripes pattern may be different depending on the thermal history. The same kind of behavior was also observed during temperature cycling on thicker samples.[25]

B. Surface morphology

We will now examine the MnAs surface morphology that is not directly related with the α-β phase transition, an issue that has not been the subject of much attention yet. In what follows, we will show that the morphology of MnAs epilayers is peculiar. A closer inspection of Fig. 2 reveals the existence of a modulation along the [0001] direction (MnAs *c*

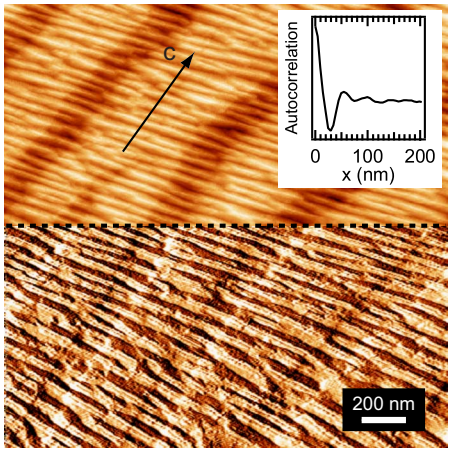

FIG. 6. (Color online) 2.0×2.0 μm^2 STM image ($I=0.5$ nA, $V_{bias}=0.8$ V) recorded at room temperature of a 130-nm-thick MnAs film epitaxied on GaAs(001), grown at 260 °C, showing the presence of elongated structures running perpendicular to the c axis of MnAs. The lowest part of the image (below the dashed line) is displayed in derivative mode in order to enhance the corrugation perpendicular to the c axis with respect to the elastic α-β modulation. Inset: autocorrelation along the c-axis direction, showing well-defined oscillations.

axis) with a submicron period. This modulation has been observed for all epilayer thicknesses in a more or less pronounced way. It is clearly observed in Fig. 6 for a 130-nm-thick sample. It is independent of the α-β domain structure, as shown in the lower part of Fig. 6 displayed in derivative mode. This data treatment amplifies sharp height variations and so enhances the contrast of the modulation of interest here at the expense of the soft α-β height profile. The autocorrelation profile obtained in the c-axis direction differs strongly from the damped function associated with roughening and exhibits a well-defined oscillatory behavior, indicating the presence of a periodic modulation. Such modulation was also evidenced by recent x-ray resonant magnetic scattering measurements that confirm its independence from the elastic stripe pattern.[20]

Smaller scale imaging of a 70-nm-thick sample reveals the presence of loosely arranged elongated pyramidal mounds [Fig. 7(a)]. These mounds are elongated along the a axis with an aspect ratio close to 5. As shown by the height profile in Fig. 7(b), they are formed by a piling of terraces with measured steps height of 0.3 nm corresponding to half-unit cell of MnAs ($a\sqrt{3}/2=0.322$ nm with $a=0.372$ nm).

Comparing the morphology at two distinct thicknesses, 130 and 70 nm (Fig. 6 and 7, respectively), one can note both slight differences and common trends. First, while the mounds display a well-defined periodicity along the [0001] direction (c axis), the arrangement is highly disordered along the perpendicular (a-axis) direction. The mounds seem to be more continuous along the a axis for thicker films. The situation is different along the c axis, where the mounds show periodical distribution and a closer inspection reveals that the majority of these objects adopt a mean slope of $10\pm1\%$ along c, corresponding to a miscut angle of $5.7\pm0.6°$. This corresponds to $5c$ or $6c$ ($c=5.72$ Å, lattice parameter along the c axis) wide terraces separated by steps running along a, as illustrated by the ball model in Fig. 7(c) that considers an ideally truncated As-terminated surface, in the absence of reconstruction and relaxation.

After postgrowth annealing under As pressure, the mounds tend to disappear and the surface morphology is smoother with the presence of larger terraces, as shown in Fig. 8. These results show that the surface morphology can be tuned through annealing. This smoothing procedure was employed, during 10 min at 300 °C, before imaging the surface depicted in Fig. 4 in order to follow the elastic modulation of the surface locally in real time. The control of the growth temperature in the 260–300 °C range should also provide a way to tailor the surface morphology. Indeed, growth at 315 °C leads to smoother surfaces with micron-size terraces.[26]

The fact that postgrowth annealing and/or growth at higher temperature considerably suppress the faceting process observed at lower temperature indicates that the facets' formation has some kinetic origin. The characteristic size of the terraces in the c-axis direction increases after annealing

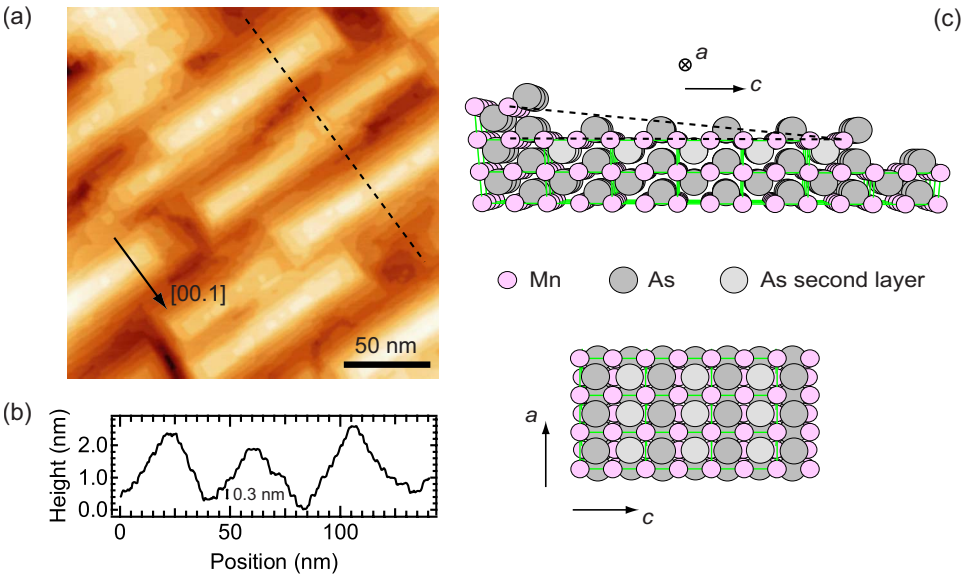

FIG. 7. (Color online) (a) 215×215 nm^2 STM image recorded at room temperature of a 70-nm-thick MnAs film epitaxied on GaAs(001), showing the presence of elongated mounds perpendicular to the c axis of MnAs. (b) Height profile across three pyramids, along the dashed line in (a), showing MnAs steps. (c) Schemes of MnAs crystal structure with steps along the c axis and perpendicular to it. The crystal has been truncated with As termination without taking into account reconstructions and relaxations.

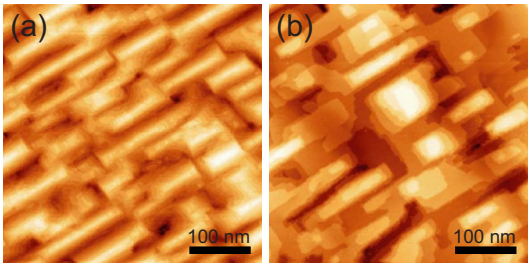

FIG. 8. (Color online) STM images recorded at room temperature of a 70-nm-thick MnAs film epitaxied on GaAs(001) grown at 260 °C (a) before annealing and (b) after annealing at 300 °C.

or growth at higher temperature. This can be understood as a consequence of an interlayer transport partially suppressed at lower temperature. The anisotropic structure of the surface could be the consequence of such a kinetic limitation, together with different sticking coefficients for steps oriented along *a* and *c*.

Whether the formation of a periodic modulation along *c* is an entirely kinetic process or is the result of a subtle balance between kinetics and thermodynamics remains an open question. Indeed, the formation of periodic structures is often observed in systems with competing short-range and long-range interactions.[27] On the other hand, kinetic limitations have been invoked in the literature to explain the formation of faceting mounds. The balance between suppressed interlayer transport due to the Ehrlich-Schwoebel barrier[28,29] and crystalline effects have been invoked to explain slope selection in mounds formation,[30] as observed in the case of homoepitaxial growth of metals, e.g., Cu growth on Cu(001) substrates where (113) and (115) facets were observed.[31] Periodic faceting in homoepitaxy of Fe on Fe(110) was also explained on kinetics grounds by Albrecht *et al.*[32] In the present case, further studies are needed to clarify the origin of the periodic faceting.

To conclude we would like to emphasize that the peculiar surface morphology described in this work might be interesting for the growth of thin films with requirements of specific substrate anisotropy. This anisotropic surface combines two kinds of modulation. The first one, in the tenth of nanometers range, is robust against temperature. The second one, perpendicular to the latter, leads to a temperature-dependent modulation of the magnetic properties (through elastic-energy minimization). It is potentially interesting as a template in order to tailor the magnetic anisotropy of a deposited ferromagnetic material. This has been recently demonstrated for Fe grown on MnAs/GaAs(001).[20,33] Iron has shown an interesting and unexpected magnetic coupling with the MnAs underlayer.

IV. CONCLUSION

The coexistence of α/β domains in MnAs/GaAs(001) epilayers has been studied by variable-temperature STM. The linear relationship between the period of the α-β-stripes pattern and the epilayer thickness has been confirmed. The height difference between α and β domains is fully coherent with the elastic origin of the pattern. High-resolution imaging during the transition rules out mass transport during the evolution of the α-β domains. Independently from the phase-transition-related long-range elastic modulation, the surface is composed of anisotropic mounds. Along the *c*-axis direction, these mounds are quasiperiodic and adopt well-defined slope. The possibility to control the periodicity of the surface morphology on different length scales makes MnAs/GaAs(001) an interesting template for the growth of anisotropic magnetic structures.

ACKNOWLEDGMENTS

We thank E. Charron for assistance in AFM measurements and M. Sacchi for enlightening and stimulating discussions. I.L. Graff wishes to thank CAPES Agency for the post-doc grant (Process No. 0532/07-0). This work is partially supported by the French Agence Nationale pour la Recherche (ANR) contract MOMES and C'Nano-IdF (project TRIPEPS).

*Present address: Departamento de Física-UFPR, CP 19044, 81531-990 Curitiba, Brazil.

[1] B. T. M. Willis, H. P. Rooksby, Proc. Phys. Soc. London, Sect. B **67**, 290(1954).
[2] R. H. Wilson and J. S. Kasper, Acta Crystallogr. **17**, 95 (1964).
[3] M. Tanaka, J. P. Harbison, T. Sands, T. L. Cheeks, V. G. Keramides, and G. M. Rothberg, J. Vac. Sci. Technol. B **12**, 1091 (1994).
[4] M. Tanaka, J. P. Harbison, M. C. Park, Y. S. Park, T. Shin, and G. M. Rothberg, J. Appl. Phys. **76**, 6278 (1994).
[5] M. Tanaka, Physica E **2**, 372 (1998).
[6] L. Däweritz, Rep. Prog. Phys. **69**, 2581 (2006).
[7] J. Varalda, A. J. A. de Oliveira, A. Ouerghi, M. Eddrief, M. Marangolo, D. Demaille, V. H. Etgens, N. Mattoso, and D. H. Mosca, J. Appl. Phys. **100**, 093524 (2006).
[8] V. Garcia, H. Jaffrès, M. Eddrief, M. Marangolo, V. H. Etgens, J.-M. George, Phys. Rev. B **72**, 081303(R) (2005).
[9] V. Garcia, H. Jaffrès, J.-M. George, M. Marangolo, M. Eddrief, and V. H. Etgens, Phys. Rev. Lett. **97**, 246802 (2006).
[10] V. M. Kaganer, B. Jenichen, F. Schippan, W. Braun, L. Däweritz, and K. H. Ploog, Phys. Rev. B **66**, 045305 (2002).
[11] V. Garcia, Y. Sidis, M. Marangolo, F. Vidal, M. Eddrief, P. Bourges, F. Maccherozzi, F. Ott, G. Panaccione, and V. H. Etgens, Phys. Rev. Lett. **99**, 117205 (2007).
[12] D. H. Mosca, F. Vidal, and V. H. Etgens, Phys. Rev. Lett. **101**, 125503 (2008).
[13] C. Adriano, C. Giles, O. D. D. Couto, M. J. S. P. Brasil, F. Iikawa, and L. Däweritz, Appl. Phys. Lett. **88**, 151906 (2006).
[14] M. Kästner, C. Herrmann, L. Däweritz, and K. H. Ploog, J. Appl. Phys. **92**, 5711 (2002).
[15] T. Plake, M. Ramsteiner, V. M. Kaganer, B. Jenichen, M. Kästner, L. Däweritz, and K. H. Ploog, Appl. Phys. Lett. **80**, 2523

(2002).
[16] M. Kästner, F. Schippan, P. Schützendübe, L. Däweritz, and K. H. Ploog, J. Vac. Sci. Technol. B **18**, 2052 (2000).
[17] R. Magalhães-Paniago, L. N. Coelho, B. R. A. Neves, H. Westfahl, F. Iikawa, L. Daweritz, C. Spezzani, and M. Sacchi, Appl. Phys. Lett. **86**, 053112 (2005).
[18] F. Vidal, O. Pluchery, N. Witkowski, V. Garcia, M. Marangolo, V. H. Etgens, and Y. Borensztein, Phys. Rev. B **74**, 115330 (2006).
[19] B. Gallas, J. Rivory, H. Arwin, F. Vidal, and M. Stchakovsky, Phys. Status Solidi A **205**, 863 (2008).
[20] M. Sacchi, M. Marangolo, C. Spezzani, L. Coelho, R. Breitwieser, J. Milano, and V. H. Etgens, Phys. Rev. B **77**, 165317 (2008).
[21] T. Arai, M. Suzuki, Y. Ueno, J. Okabayashi, and J. Yoshino, J. Cryst. Growth **301-302**, 22 (2007).
[22] I. Horcas, R. Fernandez, J. M. Gomez-Rodriguez, J. Colchero, J. Gomez-Herrero, and A. M. Baro, Rev. Sci. Instrum. **78**, 013705 (2007).
[23] D. K. Satapathy, V. M. Kaganer, B. Jenichen, W. Braun, L. Däweritz, and K. H. Ploog, Phys. Rev. B **72**, 155303 (2005).
[24] L. Däweritz, M. Kästner, T. Hesjedal, T. Plake, B. Jenichen, and K. H. Ploog, J. Cryst. Growth **251**, 297 (2003).
[25] See EPAPS Document No. E-PRBMDO-80-009928 for the surface evolution of a 280-nm-thick sample during temperature cycling in the α-β-coexistence region. For more information on EPAPS, see htpp://www.aip.org/pubservs/epaps.html.
[26] L. Däweritz and C. Herrmann, Phys. Status Solidi B **244**, 2936 (2007).
[27] M. Seul and D. Andelman, Science **267**, 476 (1995).
[28] G. Ehrlich and F. Hudda, J. Chem. Phys. **44**, 1039 (1966).
[29] R. L. Schwoebel and E. J. Shipsey, J. Appl. Phys. **37**, 3682 (1966).
[30] M. Siegert and M. Plischke, Phys. Rev. Lett. **73**, 1517 (1994).
[31] H.-J. Ernst, F. Fabre, R. Folkerts, and J. Lapujoulade, Phys. Rev. Lett. **72**, 112 (1994).
[32] M. Albrecht, H. Fritzsche, and U. Gradmann, Surf. Sci. **294**, 1 (1993).
[33] R. Breitwieser, M. Marangolo, J. Lüning, N. Jaouen, L. Joly, M. Eddrief, V. H. Etgens, and M. Sacchi, Appl. Phys. Lett. **93**, 122508 (2008).